Controlling the motional quality factor of a diamagnetically levitated graphite plate

RESEARCH ARTICLE | FEBRUARY 28 2023

Controlling the motional quality factor of a diamagnetically levitated graphite plate

P. Romagnoli; R. Lecamwasam; S. Tian; ... et. al

Appl. Phys. Lett. 122, 094102 (2023)
https://doi.org/10.1063/5.0133242

Applied Physics Letters ARTICLE scitation.org/journal/apl

Controlling the motional quality factor of a diamagnetically levitated graphite plate

Cite as: Appl. Phys. Lett. **122**, 094102 (2023); doi: 10.1063/5.0133242
Submitted: 2 November 2022 · Accepted: 7 February 2023 ·
Published Online: 28 February 2023

P. Romagnoli,[1] R. Lecamwasam,[1] S. Tian,[1] J. E. Downes,[2] and J. Twamley[1,a)]

AFFILIATIONS

[1]Quantum Machines Unit, Okinawa Institute of Science and Technology Graduate University, Onna, Okinawa 904-0495, Japan
[2]School of Mathematical and Physical Science, Macquarie University, Sydney 2109, New South Wales, Australia

[a)]Author to whom correspondence should be addressed: jason.twamley@oist.jp

ABSTRACT

Researchers seek methods to levitate matter for a wide variety of purposes, ranging from exploring fundamental problems in science through to developing new sensors and mechanical actuators. Many levitation techniques require active driving and most can only be applied to objects smaller than a few micrometers. Diamagnetic levitation has the strong advantage of being the only form of levitation which is passive, requiring no energy input, while also supporting massive objects. Known diamagnetic materials which are electrical insulators are only weakly diamagnetic and require large magnetic field gradients to levitate. Strong diamagnetic materials which are electrical conductors, such as graphite, exhibit eddy damping, restricting motional freedom and reducing their potential for sensing applications. In this work, we describe a method to engineer the eddy damping while retaining the force characteristics provided by the diamagnetic material. We study, both experimentally and theoretically, the motional damping of a magnetically levitated graphite plate in high vacuum and demonstrate that one can control the eddy damping by patterning the plate with through-slots which interrupt the eddy currents. We find that we can control the motional quality factor over a wide range with excellent agreement between the experiment and numerical simulations.

The levitation of matter has a variety of applications ranging from quantum science and technology through to industrial development of levitated actuators, motors, and robots. Typically to levitate or trap an object requires a source of power, e.g., optical trapping uses strong laser fields, while dynamic electric fields can hold charged objects in Paul traps. These so-called "active" systems suffer from various types of noise and thereby motional heating. In contrast, "passive" diamagnetic levitation, which requires no active driving or energy input, has the potential for very low noise, low heating, levitation, and motional control. Moreover, macroscopic objects can easily be supported and manipulated.[1] For this reason, diamagnetic levitation has recently attracted much attention and since its original exposition,[2–7] it is now firmly regarded as one of the main techniques in *levitodynamics*.[8–10]

Levitation can be used to explore many fundamental questions, including testing ideas in thermodynamics[11] and alternative theories of quantum mechanics,[12] and searching for new types of forces in nature.[13–15] Tabletop experiments have been proposed which explore the relationship between quantum theory and gravity.[16–21] Another major application of levitodynamics is the development of novel sensors, including inertial sensors,[22–27] detecting gravitational waves[28] and dark matter/energy,[29] magnetometry,[30] measuring mass,[31] and light pressure sensing.[32] It is only in levitated systems (using optical trapping) that a macroscopic quantum superposition has ever been achieved.[33–36] Within levitodynamics, plates of pyrolytic graphite are gaining increasing attention as a highly promising platform. These have already been used to experimentally test theories of dark matter[29] and may outperform other types of levitated systems.[37]

In addition to quantum science, another important area of levitodynamics is the development of levitated actuators, motors, and robots. These typically use magnetic levitation, due to its ability to support large mass loads against gravity. An example includes the development of miniature robots which move on a planar surface and can be controlled via localized currents.[38–42] Researchers have recently developed photo-thermal methods to actuate the motion of a diamagnetically levitated graphite plate, which has led to a large interest in developing photo-activated 2D positioners.[43–50] We particularly note recent works using diamagnetic levitated graphite for optical energy harvesting,[51] and a multiple-degree-of-freedom nanopositioner.[52]

For diamagnetic levitation of macroscopic masses, for example, those used in actuators, the ideal material is Highly Oriented Pyrolytic Graphite (HOPG) due to its extremely high magnetic susceptibility normal to the slab face.[1,53] However, HOPG is an excellent conductor; thus, eddy currents are induced as it moves through magnetic fields. These cause damping, reducing the quality factor of the motional mode, and producing heat leading to thermal noise. Higher quality factors may be achieved in materials which are electrical insulators, such as diamond, polymers, some glasses, and organic materials.[27,54,55] However, these tend to be only weakly diamagnetic,[6,56] thus unsuited to levitation of centimeter-sized objects (see Sec. I of the supplementary material for a brief numerical comparison).

For applications, such as robots and actuators, it may not be necessary to completely eliminate eddy damping, which may even be useful in some situations. For other applications, however, such as motional sensors, it is desirable to completely remove the eddy damping. In electrical transformers, engineers reduce eddy losses either by interrupting the currents with layers of laminated material or by making the core of the transformer out of a highly resistive ferrite magnetic material. The latter route was recently adapted to the diamagnetic levitation of graphite,[37] where micrometer-scale graphite particles were encapsulated in an electrically insulating resin. Eddy currents and the associated damping were significantly reduced, leading to quality a factor of 5×10^5. At the same time, however, this results in a lowering of the diamagnetic lift. The filling fraction of graphite within the resin cannot be too high without compromising structural integrity, and random orientation of the particles within the resin lowers the effective magnetic susceptibility.

In our work, we seek to control eddy damping using a method more similar to the lamination technique in electrical transformers. We consider the diamagnetic levitation of a solid slab of HOPG, which we then pattern with very narrow through-cut slots, the purpose of which is to interrupt the path of eddy currents. We machine several samples with increasing slot densities. We hypothesize that as we modify the density of slotted interruptions to the eddy currents, then these currents will be modified and so too will the associated eddy damping. The advantage of this method to control the eddy damping is that one retains virtually all the diamagnetic lift of the original HOPG slab, as the through-slots are very narrow.

In the following, we outline the experiment, analysis, and simulation of the levitodynamics of the slotted graphite plates. We find that the through-cut slots allow us to systematically control the motional quality factor in a highly predictable manner, with excellent agreement between theory and experiment.

A sketch of the experimental setup is presented in Fig. 1. A plate of pyrolytic graphite is levitated by four NdFeB magnets placed in an alternating polarity checkerboard pattern. The magnets are rigidly held within a holder which is fixed to a five axis vacuum-compatible motorized stage. The magnet/motor platform is mounted on a small optical breadboard which, in turn, sits on four vibration isolation supports. The position of the graphite sample is monitored by an interferometric displacement sensor. This displacement sensor is based on a compact Michelson interferometer and enables high precision measurements in real time with a resolution of picometers at a high bandwidth.

The whole structure is positioned in a vacuum chamber, which is evacuated by a system consisting of a turbopump, an ion pump, and

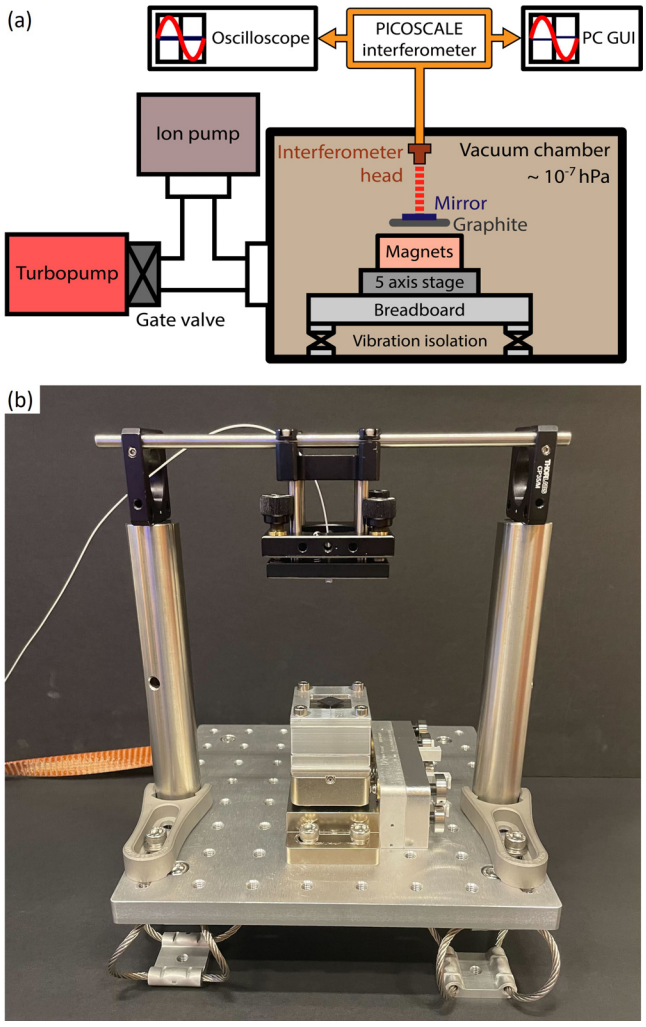

FIG. 1. Experimental setup. (a) A plate of pyrolitic graphite is levitated by four NdFeB N52 magnets with polarities arranged in a checkerboard pattern. The magnets are fixed on a five-axis motorized stage, which is supported by a breadboard resting upon four vibration isolation mounts within the vacuum chamber. The vacuum chamber and ion pump lie on a vibration isolation optical table, while the turbopump is on a separate vibration isolation platform. A small mirror is fixed to the graphite sample, which is used by an interferometer to measure the vertical displacement. The interferometer is aligned using the five-axis stage. (b) Photograph of the platform which sits inside the vacuum chamber.

associated roughing pump. During the measurement periods, the turbopump is switched off to avoid unwanted mechanical vibrations, while the ion-pump operates continuously to maintain high vacuum (10^{-7} hPa). The vacuum chamber and ion pump are supported by a damped and vibration isolated optical table, while the turbopump is supported by a separate vibration damped and isolated platform.

The experiment aims to increase the motional quality factor of a diamagnetically levitated slab of pyrolytic graphite. Four 10×10 mm^2 samples were machined from a single piece of graphite, to ensure that they all possessed similar electric and magnetic properties. The thickness of each sample was approximately 0.77 mm; however, this was

not uniform since the graphite surface was very coarse. Each plate had a pattern of ring-like slits machined into it whose purpose was to interrupt the eddy currents and hence lower the resulting eddy damping forces. These slits were created by femtosecond laser machining. The slit designs and photographs of the machined samples are shown in Fig. 2. A small mirror was then glued onto the center of each piece, to allow an interferometer to measure vertical displacement. Each graphite sample was levitated for a period of 20 min, and its vertical position was recorded using the interferometer. The resulting power spectral density was then analyzed to find the motional quality factor. Further details of the setup are given in Sec. II of the supplementary material.

Due to its positioning, the interferometer is most sensitive to vertical motion of the plate. To understand the frequencies observed in the experiment, we simulated the motional modes for the $N = 0$ plate. These modes are determined by the forces and torques experienced as it moves through the inhomogeneous magnetic field above the magnet array. As discussed in Sec. IV of the supplementary material and in agreement with Chen *et al.*,[1] there are six modes in total. Three of them, oscillations in the horizontal plane or rotation about the vertical axis, have frequencies bunched around 4 Hz. The other three involve vertical motion, namely, vertical oscillation and tilting about the horizontal axes and are predicted to have frequencies around 17 Hz. It is these vertical modes that our interferometric setup will be most sensitive to.

As the graphite plate moves, the magnetic field it experiences, and hence the magnitude and direction of the force on the plate, varies in a complex manner. This will cause a nontrivial coupling between all of the motional modes. For simplicity, we will approximate the three vertical modes as a single effective mode of a one-dimensional oscillator. This oscillator is primarily damped by eddy currents, induced by motion of the plate through the magnetic field. Damping due to air should be negligible at the pressures we consider, see Sec. IV of the supplementary material for detailed calculation.

The power spectral density for a harmonic oscillator is given in Sec. X of Ref. 57. As discussed in Sec. V of the supplementary material, the power spectral densities for the experimental data traces were fitted to the theoretical values, allowing us to extract the effective damping rates γ and natural frequencies f_0, from which we could calculate the quality factor Q of each oscillator. These are shown in Fig. 3.

As expected, the oscillation frequencies are all approximately 17 Hz. Moreover, there is a slight upward shift in f_0 as the number of slots increases. As discussed in Sec. IV of the supplementary material, simulations indicate that this is due to the inhomogeneous removal of material from the graphite plate. In total, the rings are able to increase the oscillator quality factor by a factor of $\sim$40.

To estimate the expected increase in the quality factor due to the slits, we simulated the eddy currents in each of the graphite plates in Fig. 2. The currents are induced by an effective electric potential which depends on the geometry of the plate and its motion through the external magnetic field.[1,58–60] This current then exerts a force on the plate due to the magnetic field, which can be integrated to find the induced eddy damping. We developed both a two-dimensional model in Mathematica and three-dimensional COMSOL simulation, the details of which are described in Sec. VI of the supplementary material.

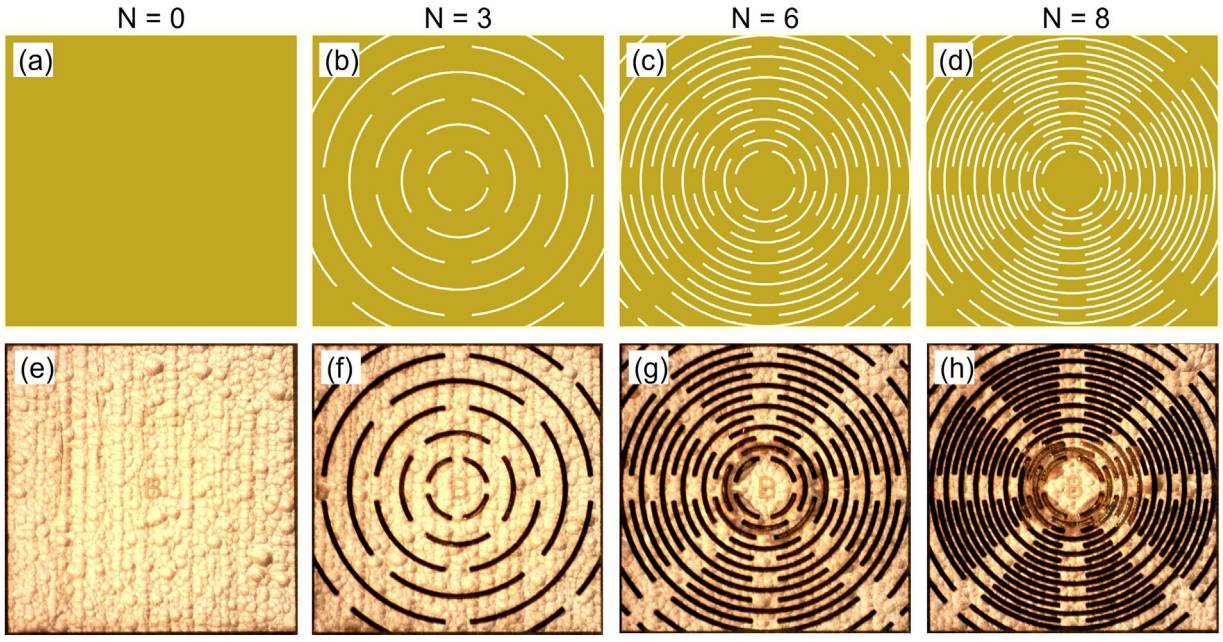

FIG. 2. Slit designs and photographs of the machined graphite samples. (a)–(d) CAD design patterns of ring-like slits. These are named $N = 0$, 3, 6, and 8, with N reflecting a parameter used to generate the ring patterns. As N grows larger slit density increases, leading to stronger suppression of eddy currents and an increase in the motional quality factor. (e)–(h) Photos of the machined graphite plates, measuring $10 \times 10\,\text{mm}^2$. The thickness is approximately 0.77 mm; however, this is not uniform due the visible surface roughness. After machining, a mirror (not shown, made from aluminum coating on glass) was glued to the center of each plate for optical measurement of the motion.

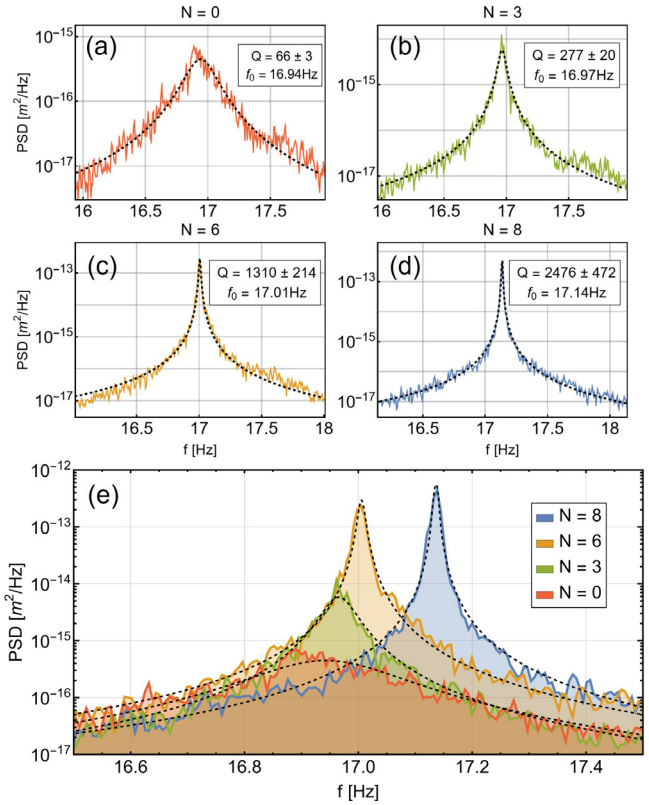

FIG. 3. Power spectral density of the vertical motion. In (a)–(d) the solid, colored traces show the experimental data. The dashed black line denotes the theoretical fit, with insets showing the fitted quality factors (Q) and resonance frequencies (f_0). Errors come from the covariance matrix of the fit. With increased slit density, the quality factor increases from $Q_{N=0} \sim 66$ to $Q_{N=8} \sim 2476$. In (e), we overlap the power spectral densities. As the number of slits increases, the resonance peaks get sharper, and there is a slight increase in frequency.

The two-dimensional model used the finite element method in Mathematica 13.0 to simulate the currents. Moving from $N = 0$ to $N = 8$, the total current was found to have decreased by an order of magnitude. Around the edges of a slit, very large currents could occur, however, as these occur in infinitesimal areas they do not contribute significantly to eddy damping.

At low pressures, eddy currents are solely responsible for motional damping γ_{eddy} of the plate. The quality factor of a mode is inversely proportional to the damping rate: $q_N \propto m_N/\gamma_{\text{eddyn}}$, for sample N with mass m_N. Hence, we can predict the ratio of quality factors of the different plates, by calculating the ratios of their corresponding γ_{eddy} values and masses. These are shown in Fig. 4. We can see that the simulated values agree well with experiment. The $N = 8$ sample does appear to have a slightly larger quality factor than predicted, which as we will discuss later is most likely due to the machined slots being wider than the design.

We also built a three-dimensional model using the commercial FEM package COMSOL. The eddy currents are plotted in Fig. 5 (these do not significantly differ from those generated in Mathematica). Using this, we were able to predict the absolute values of the quality

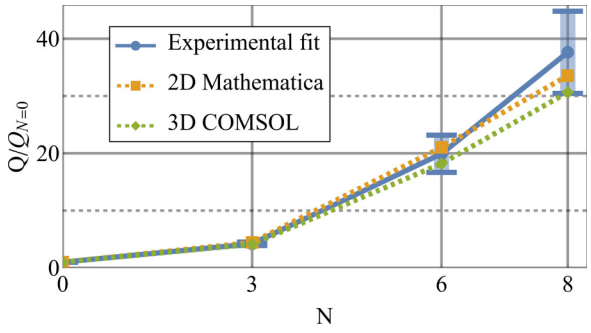

FIG. 4. Plate quality factors relative to $N = 0$. The solid blue trace is obtained from fitting the experimental power spectral density. The dashed lines show the simulated quality factors due to eddy damping. The orange trace shows the two-dimensional model in Mathematica, while the green is the three-dimensional COMSOL model. The simulations are all within experimental error, indicating that the observed increase in the quality factor is due to suppression of eddy currents.

factors, rather than simply their ratios. The results of the COMSOL simulation are also plotted in Fig. 4, agreeing with the results from the experiment and Mathematica.

The motional quality factor of the graphite plates was measured to increase as more slots were cut into the surface. This increase was consistent with both the two-dimensional Mathematica and three-dimensional COMSOL simulations of the eddy current damping. This indicates that the increase in the quality factor is, indeed, due to suppression of eddy currents. Overall currents were suppressed by an order of magnitude, corresponding to an increase in a quality factor of 40.

In Fig. 4, we can see that for $N = 8$, the simulated quality factors are slightly lower than the experimental value. We attribute this primarily to a discrepancy between the designed slot patterns and what is created by the femtosecond laser cutting. In Fig. 2, the slot patterns of the laser-cut samples are clearly wider than the CAD designs. Moreover, the machining process carves V-shaped slits which remove more graphite than expected, an effect which is more pronounced at high slit density. Wider slots yield less eddy currents and, thus, reduced eddy damping, leading to higher quality factors in the actual samples than what is predicted by our models.

To motivate the design of future systems, we explore a simple analytic model of a conductive metal plate oscillating above a cylindrical magnet in Sec. VII of the supplementary material. The quality factor is found to be inversely proportional to conductivity, independent of plate thickness, and proportional to $1/a^2$, where a is the length of the plate.

Pyrolytic graphite is one of the most strongly diamagnetic materials known and has great potential for use in levitated technologies. However, due to its high electrical conductivity, it exhibited strong eddy damping. The ability to engineer this damping while retaining a strong diamagnetic susceptibility will permit researchers in a wide range of disciplines the ability to apply such conducting diamagnetic materials to situations where fast motional control is required. We showed that by patterning the graphite plate with through-slots, we can interrupt the eddy currents in a controlled manner and gain detailed control over the eddy damping while retaining the strong

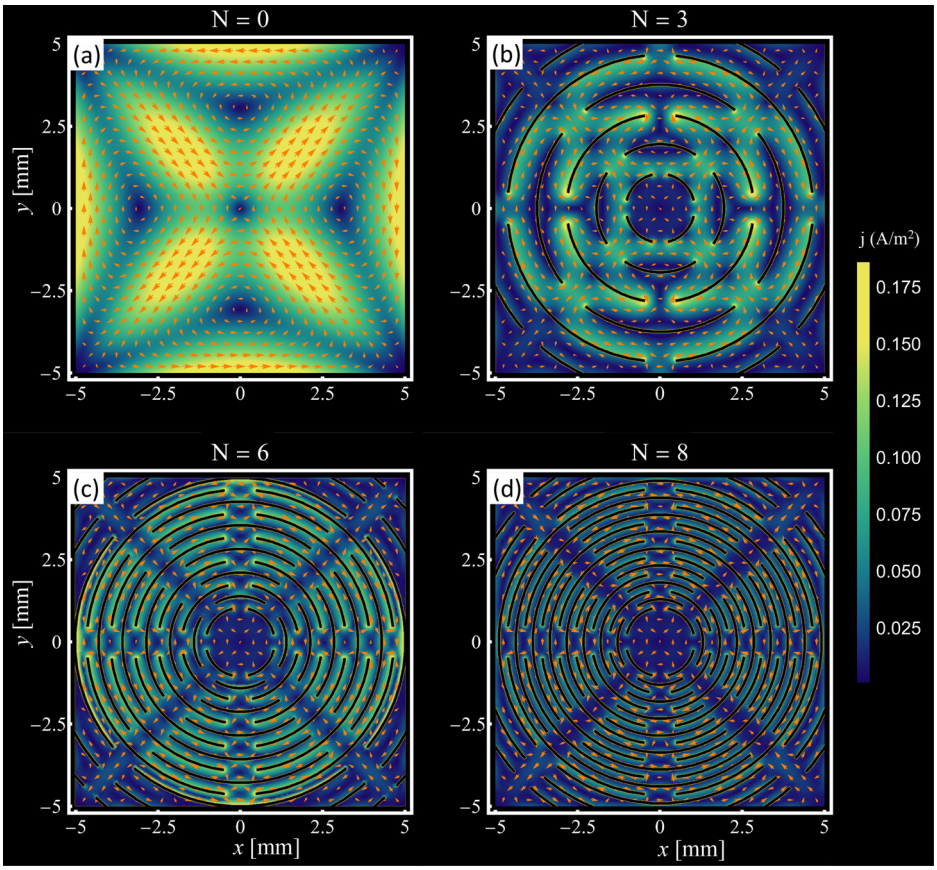

FIG. 5. Eddy currents simulated by COMSOL on the bottom surface of each plate. The plate is assumed to move vertically downward away from its equilibrium position. The currents simulated by the two-dimensional Mathematica model are similar. We choose $v = -6 \times 10^{-6}$ m/s for $n = 0$ and $N = 3$ and $v = -12 \times 10^{-6}$ m/s for $N = 6$ and $N = 8$ (the different velocities are to ensure the currents are still visible at higher N values). The color denotes the current magnitude, while arrows show the current direction. Around the edges of the slits, the current can attain very large values not shown on our color scale, but these occur in vanishingly small regions. As the number of slits increases, the eddy currents are significantly suppressed.

diamagnetic lift. In this study, we have not optimized the slotted pattern, and it is an interesting question whether one can produce designs which remove the least material, maintain the structural integrity of the plate, and control the eddy damping to the maximal extent.

See the supplementary material for a discussion about the comparison with diamagnetic electrical insulators, details of the experimental setup, the laser machining setup, analysis of the motional mode frequencies, power spectral density, and eddy damping both numerically and analytically.

This work was supported by the Okinawa Institute of Science and Technology Graduate University, Japan and Macquarie University, Sydney, Australia. The authors acknowledge the technical assistance from A. Elarabi and P. Kennedy from the OIST Engineering Section. The graphite slab machining work was performed in part at the OptoFab node of the Australian National Fabrication Facility (ANFF) utilizing Commonwealth and NSW State Government funding.

AUTHOR DECLARATIONS

Conflict of Interest

The authors have no conflicts to disclose.

Author Contributions

P. Romagnoli, R. Lecamwasam, and S. Tian contributed equally to this work.

Priscila Romagnoli: Conceptualization (equal); Data curation (equal); Formal analysis (equal); Investigation (equal); Writing – original draft (equal); Writing – review & editing (equal). **Ruvindha Lecamwasam:** Conceptualization (equal); Formal analysis (equal); Investigation (equal); Methodology (equal); Software (equal); Writing – original draft (equal); Writing – review & editing (equal). **Shilu Tian:** Conceptualization (equal); Formal analysis (equal); Investigation (equal); Methodology (equal); Software (equal); Writing – original draft (equal); Writing – review & editing (equal). **James E. Downes:** Conceptualization (equal); Investigation (equal); Methodology (equal); Writing – original draft (equal); Writing – review & editing (equal). **Jason Twamley:** Conceptualization (equal); Formal analysis (equal); Investigation (equal); Methodology (equal); Project administration (equal); Software (equal); Supervision (equal); Writing – original draft (equal); Writing – review & editing (equal).

DATA AVAILABILITY

The data that support the findings of this study are available from the corresponding author upon reasonable request.

REFERENCES

[1]X. Chen, A. Keşkekler, F. Alijani, and P. G. Steeneken, "Rigid body dynamics of diamagnetically levitating graphite resonators," Appl. Phys. Lett. **116**, 243505 (2020).
[2]W. Thomson, "On the forces experienced by small spheres under magnetic influence; and on some of the phenomena presented by diamagnetic substances," Cambridge Dublin Math. J. **2**, 499–505 (1847).
[3]W. Thomson, "Remarks on the forces experienced by inductively magnetized ferromagnetic or diamagnetic non-crystalline substances," London, Edinburgh, Dublin Philos. Mag. J. Sci. **37**, 241–253 (1850).
[4]W. Braunbek, "Freies Schweben diamagnetischer Körper im magnetfeld," Z. Phys. **112**, 764–769 (1939).
[5]M. V. Berry and A. K. Geim, "Of flying frogs and levitrons," Eur. J. Phys. **18**, 307–313 (1997).
[6]M. D. Simon and A. K. Geim, "Diamagnetic levitation: Flying frogs and floating magnets (invited)," J. Appl. Phys. **87**, 6200–6204 (2000).
[7]M. D. Simon, L. O. Heflinger, and A. K. Geim, "Diamagnetically stabilized magnet levitation," Am. J. Phys. **69**, 702–713 (2001).
[8]C. Gonzalez-Ballestero, M. Aspelmeyer, L. Novotny, R. Quidant, and O. Romero-Isart, "Levitodynamics: Levitation and control of microscopic objects in vacuum," Science **374**, eabg3027 (2021).
[9]Q. Gao, H. Yan, H. Zou, W. Li, Z. Peng, G. Meng, and W. Zhang, "Magnetic levitation using diamagnetism: Mechanism, applications and prospects," Sci. China Technol. Sci. **64**, 44–58 (2021).
[10]J. Millen and B. A. Stickler, "Quantum experiments with microscale particles," Contemp. Phys. **61**, 155–168 (2020).
[11]J. Gieseler and J. Millen, "Levitated nanoparticles for microscopic thermodynamics—A review," Entropy **20**, 326 (2018).
[12]A. Pontin, N. P. Bullier, M. Toroš, and P. F. Barker, "Ultranarrow-linewidth levitated nano-oscillator for testing dissipative wave-function collapse," Phys. Rev. Res. **2**, 023349 (2020).
[13]D. C. Moore and A. A. Geraci, "Searching for new physics using optically levitated sensors," Quantum Sci. Technol. **6**, 014008 (2021).
[14]F. Xiong, T. Wu, Y. Leng, R. Li, C.-K. Duan, X. Kong, P. Huang, Z. Li, Y. Gao, X. Rong, and J. Du, "Searching spin-mass interaction using a diamagnetic levitated magnetic-resonance force sensor," Phys. Rev. Res. **3**, 013205 (2021).
[15]C. Timberlake, A. Vinante, F. Shankar, A. Lapi, and H. Ulbricht, "Probing modified gravity with magnetically levitated resonators," Phys. Rev. D **104**, L101101 (2021).
[16]S. Bose, A. Mazumdar, G. W. Morley, H. Ulbricht, M. Toroš, M. Paternostro, A. A. Geraci, P. F. Barker, M. S. Kim, and G. Milburn, "Spin entanglement witness for quantum gravity," Phys. Rev. Lett. **119**, 240401 (2017).
[17]C. Marletto and V. Vedral, "Gravitationally induced entanglement between two massive particles is sufficient evidence of quantum effects in gravity," Phys. Rev. Lett. **119**, 240402 (2017).
[18]M. Christodoulou and C. Rovelli, "On the possibility of laboratory evidence for quantum superposition of geometries," Phys. Lett. B **792**, 64–68 (2019).
[19]M. Carlesso, A. Bassi, M. Paternostro, and H. Ulbricht, "Testing the gravitational field generated by a quantum superposition," New J. Phys. **21**, 093052 (2019).
[20]H. C. Nguyen and F. Bernards, "Entanglement dynamics of two mesoscopic objects with gravitational interaction," Eur. Phys. J. D **74**, 2–6 (2020).
[21]R. J. Marshman, A. Mazumdar, R. Folman, and S. Bose, "Constructing nano-object quantum superpositions with a Stern-Gerlach interferometer," Phys. Rev. Res. **4**, 023087 (2022).
[22]D. Garmire, H. Choo, R. Kant, S. Govindjee, C. H. Séquin, R. S. Muller, and J. Demmel, "Diamagnetically levitated MEMS accelerometers," in *TRANSDUCERS and EUROSENSORS '07—4th International Conference on Solid-State Sensors, Actuators and Microsystems* (IEEE, 2007), pp. 1203–1206.
[23]D. Hempston, J. Vovrosh, M. Toroš, G. Winstone, M. Rashid, and H. Ulbricht, "Force sensing with an optically levitated charged nanoparticle," Appl. Phys. Lett. **111**, 133111 (2017).
[24]J. Prat-Camps, C. Teo, C. C. Rusconi, W. Wieczorek, and O. Romero-Isart, "Ultrasensitive inertial and force sensors with diamagnetically levitated magnets," Phys. Rev. Appl. **8**, 034002 (2017).
[25]C. Timberlake, G. Gasbarri, A. Vinante, A. Setter, and H. Ulbricht, "Acceleration sensing with magnetically levitated oscillators above a superconductor," Appl. Phys. Lett. **115**, 224101 (2019).
[26]F. Monteiro, W. Li, G. Afek, C. L. Li, M. Mossman, and D. C. Moore, "Force and acceleration sensing with optically levitated nanogram masses at microkelvin temperatures," Phys. Rev. A **101**, 53835 (2020).
[27]C. W. Lewandowski, T. D. Knowles, Z. B. Etienne, B. D'Urso, and B. D'Urso, "High-sensitivity accelerometry with a feedback-cooled magnetically levitated microsphere," Phys. Rev. Appl. **15**, 014050 (2021).
[28]A. Arvanitaki and A. A. Geraci, "Detecting high-frequency gravitational waves with optically levitated sensors," Phys. Rev. Lett. **110**, 071105 (2013).
[29]P. Yin, R. Li, C. Yin, X. Xu, X. Bian, H. Xie, C.-K. Duan, P. Huang, J.-H. He, and J. Du, "Experiments with levitated force sensor challenge theories of dark energy," Nat. Phys. **18**, 1181–1185 (2022).
[30]P. Kumar and M. Bhattacharya, "Magnetometry via spin-mechanical coupling in levitated optomechanics," Opt. Express **25**, 19568–19582 (2017).
[31]X. Chen, N. Kothari, A. Keşkekler, P. G. Steeneken, and F. Alijani, "Diamagnetically levitating resonant weighing scale," Sens. Actuators, A **330**, 112842 (2021).
[32]A. K. Vaskuri, D. W. Rahn, P. A. Williams, and J. H. Lehman, "Absolute radiation pressure detector using a diamagnetically levitating test mass," Optica **8**, 1380 (2021).
[33]F. Tebbenjohanns, M. Frimmer, V. Jain, D. Windey, and L. Novotny, "Motional sideband asymmetry of a nanoparticle optically levitated in free space," Phys. Rev. Lett. **124**, 13603 (2020).
[34]U. Delić, M. Reisenbauer, K. Dare, D. Grass, V. Vuletić, N. Kiesel, and M. Aspelmeyer, "Cooling of a levitated nanoparticle to the motional quantum ground state," Science **367**, 892–895 (2020).
[35]L. Magrini, P. Rosenzweig, C. Bach, A. Deutschmann-Olek, S. G. Hofer, S. Hong, N. Kiesel, A. Kugi, and M. Aspelmeyer, "Real-time optimal quantum control of mechanical motion at room temperature," Nature **595**, 373–377 (2021).
[36]F. Tebbenjohanns, M. L. Mattana, M. Rossi, M. Frimmer, and L. Novotny, "Quantum control of a nanoparticle optically levitated in cryogenic free space," Nature **595**, 378–382 (2021).
[37]X. Chen, S. K. Ammu, K. Masania, P. G. Steeneken, and F. Alijani, "Diamagnetic composites for high-Q levitating resonators," Adv. Mater. **9**(32), 2203619 (2022).
[38]R. Pelrine, A. Wong-Foy, B. McCoy, D. Holeman, R. Mahoney, G. Myers, J. Herson, and T. Low, "Diamagnetically levitated robots: An approach to massively parallel robotic systems with unusual motion properties," in *Proceedings—IEEE International Conference on Robotics and Automation* (IEEE, 2012), pp. 739–744.
[39]R. Pelrine, A. Hsu, A. Wong-Foy, B. McCoy, and C. Cowan, "Optimal control of diamagnetically levitated millirobots using automated search patterns," in *International Conference on Manipulation, Automation and Robotics at Small Scales (MARSS)* (IEEE, 2016), pp. 1–6.
[40]A. Hsu, C. Cowan, W. Chu, B. McCoy, A. Wong-Foy, R. Pelrine, C. Velez, D. Arnold, J. Lake, J. Ballard, and J. Randall, "Automated 2D micro-assembly using diamagnetically levitated milli-robots," in *International Conference on Manipulation, Automation and Robotics at Small Scales (MARSS)* (IEEE, 2017), pp. 1–6.
[41]R. Pelrine, A. Hsu, and A. Wong-Foy, "Methods and results for rotation of diamagnetic robots using translational designs," in *International Conference on Manipulation, Automation and Robotics at Small Scales (MARSS)* (IEEE, 2019), pp. 1–6.
[42]J. Kuthan, M. Jurik, M. Vitek, and F. Mach, "Collective planar actuation of miniature magnetic robots towards individual robot operation," in *International Conference on Manipulation, Automation and Robotics at Small Scales (MARSS)* (IEEE, 2020), pp. 1–6.
[43]M. Kobayashi and J. Abe, "Optical motion control of maglev graphite," J. Am. Chem. Soc. **134**, 20593–20596 (2012).
[44]B. Han, Y.-L. Zhang, Q.-D. Chen, and H.-B. Sun, "Carbon-based photothermal actuators," Adv. Funct. Mater. **28**, 1802235 (2018).
[45]M. Yang, Z. Yuan, J. Liu, Z. Fang, L. Fang, D. Yu, and Q. Li, "Photoresponsive actuators built from carbon-based soft materials," Adv. Opt. Mater. **7**, 1900069 (2019).
[46]J. Young, H. Biggs, S. Yee, and H. ElBidweihy, "Optical control and manipulation of diamagnetically levitated pyrolytic graphite," AIP Adv. **9**, 125038 (2019).

[47]M. Ewall-Wice, S. Yee, K. DeLawder, S. R. Montgomery, P. J. Joyce, C. Brownell, and H. ElBidweihy, "Optomechanical actuation of diamagnetically levitated pyrolytic graphite," IEEE Trans. Magn. **55**, 1–6 (2019).
[48]J. H. Kim, J. Pyo, and T. Kim, "Highly mobile levitating soft actuator driven by multistimuli-responses," Adv. Mater. Interfaces **7**, 2001051 (2020).
[49]Y. Huang, Q. Yu, C. Su, J. Jiang, N. Chen, and H. Shao, "Light-responsive soft actuators: Mechanism, materials, fabrication, and applications," Actuators **10**, 298 (2021).
[50]S. Yee, L. Oney, T. Cosby, D. P. Durkin, and H. ElBidweihy, "Photothermal actuation of levitated pyrolytic graphite revised," APL Mater. **9**, 101107 (2021).
[51]S. Shen, L. Wu, S. Yang, Q. Yang, J.-T. Liu, and Z. Wu, "Optical energy harvesting in vibrate maglev graphite," Carbon **187**, 266–271 (2022).
[52]K. S. Vikrant and G. R. Jayanth, "Diamagnetically levitated nanopositioners with large-range and multiple degrees of freedom," Nat. Commun. **13**, 3334 (2022).
[53]C. Niu, F. Lin, Z. M. Wang, J. Bao, and J. Hu, "Graphene levitation and orientation control using a magnetic field," J. Appl. Phys. **123**, 044302 (2018).
[54]R. Nakashima, "Diamagnetic levitation of a milligram-scale silica using permanent magnets for the use in a macroscopic quantum measurement," Phys. Lett. A **384**, 126592 (2020).
[55]Y. Leng, R. Li, X. Kong, H. Xie, D. Zheng, P. Yin, F. Xiong, T. Wu, C.-K. Duan, Y. Du, Z-q Yin, P. Huang, and J. Du, "Mechanical dissipation below 1 μHz with a cryogenic diamagnetic levitated micro-oscillator," Phys. Rev. Appl. **15**, 024061 (2021).
[56]R. Freedman and H. Young, *University Physics With Modern Physics*, 15th ed. (Pearson, 2019).
[57]M. C. Wang and G. E. Uhlenbeck, "On the theory of the Brownian motion II," Rev. Mod. Phys. **17**, 323–342 (1945).
[58]M. Kirpo, T. Boeck, and A. Thess, "Eddy-current braking of a translating solid bar by a magnetic dipole," PAMM **10**, 513–514 (2010).
[59]E. V. Votyakov and A. Thess, "Interaction of a magnetic dipole with a slowly moving electrically conducting plate," J. Eng. Math. **77**, 147–161 (2012).
[60]M. Carlstedt, K. Porzig, M. Ziolkowski, R. P. Uhlig, H. Brauer, and H. Toepfer, "Comparison of Lorentz force eddy current testing and common eddy current testing-measurements and simulations," Stud. Appl. Electromagn. Mech. **39**, 218–225 (2014).